UC San Diego
UC San Diego Previously Published Works

Title

Sawtooth-triggered limit-cycle oscillations and I-phase in the HL-2A tokamak

Permalink

Journal

ISSN

Authors

Zhao, KJ
Cheng, J
Diamond, PH
et al.

Publication Date

DOI

Copyright Information

Peer reviewed

Sawtooth-triggered limit-cycle oscillations and I-phase in the HL-2A tokamak

K. J. Zhao[1,2,3], J. Cheng[2], P. H. Diamond [1,4], J. Q. Dong[2,7], L. W. Yan[2], W. Y. Hong[2], M. Xu[4], G. Tynan[4], K. Miki[1], Z. H. Huang[2], K. Itoh[5], S. -I. Itoh[6], A. Fujisawa[6], Y. Nagashima[6], S. Inagaki[6], Z. X. Wang[8], L. Wei[8], X. M. Song[2], G. J. Lei[2], Q. Li[2], X. Q. Ji[2], Yi. Liu[2], Q. W. Yang[2], X. T. Ding[2], X. R. Duan[2] and HL-2A team

1. WCI Center for Fusion Theory, National Fusion Research Institute, Gwahangno 113, Yusung-gu, Daejeon 305-806, Korea

2. Southwestern Institute of Physics, P.O. Box 432, Chengdu, China

3. National Fusion Research Institute, Gwahangno 113, Yusung-gu, Daejeon 305-806, Korea

4. Center for Momentum Transport and Flow Organization, University of California at San Diego, California 92093, USA

5. National Institute for Fusion Science, Toki 509-5292, Japan,

6. Research Institute for Applied mechanics, Kyushu University, Kasuga, Kasuga koen 6-1, 816-8580, Japan

7. Institute for Fusion Theory and Simulation, Zhejiang University, Hangzhou, China

8. School of Physics and Optoelectronic Technology, Dalian University of Technology, Dalian 116024

Corresponding author: kjzhao@swip.ac.cn

Abstract: Transitions between low (L-mode) and intermediate (I-phase) confinement regimes triggered by sawteeth are investigated by using multiple Langmuir probe arrays in the edge plasmas of the HL-2A tokamak. The I-phase is characterized by limit cycle oscillations (LCOs). Repeated L-I-L transitions induced by sawtooth heat pulses are also observed. The statistical analyses show that the delay time of the L-I transition

relative to sawtooth crashes is less than ~1ms. The intensity of turbulence bursts in the I-phase is stronger than those observed in L-mode plasmas. Measurement are consistent with zonal flow reducing turbulence intensity in the frequency band of ~20-100 kHz, while the turbulence of frequency higher than 100 kHz has more power than that in the L-mode. The analyses of the time-resolved power transfers between turbulence and zonal flows suggest that the power transfers exist between turbulence and zonal flows and the direction of the power transfers is from turbulence into geodesic acoustic modes in ohmic plasmas.

1. Introduction

The transition from low (L-mode) to high (H-mode) state exists in various magnetic confinement fusion devices and has attracted strong interest in the fusion community in the effort to understand the dynamics of the L-H transition since it was discovered on ASDEX [1].

The L-H transition is a transport bifurcation phenomenon and characterized by turbulence suppression, reduced transport levels, and steep gradients at plasma edge due to strong ExB shear layers. Two types of flows-mean flows generated by the mean pressure gradient and time varying flows driven by nonlinear interaction via turbulent stresses, called zonal flows-contribute to the L-H transition [2-7]. With slowly increasing input power near H-mode power threshold, an intermediate, quasi-periodic state, called the I-phase, a limit cycle oscillation (LCO) or a dithering H-mode was observed [8-12]. By contrast, in the I-mode cases, the quasi-periodic state is not necessary [13]. In the I-phase, turbulence, zonal and mean flows couple with the pressure gradient [14-15]. Zonal flows are generated by turbulent stresses when turbulence becomes sufficiently strong to overcome flow damping. Inversely the zonal flow shearing suppresses turbulence and subsequently the drive for zonal flow is depleted by a mean shearing resulting from the ion pressure gradient. The zonal flow, even if only occurring in a single burst [16], can trigger the transition by regulating turbulence level and associated transport until the mean flow is high enough to suppress the remaining turbulence and sustain a steep pressure gradient.

However, the triggering physics, which is crucial for the International Thermonuclear Experimental Reactor (ITER) to access the H-mode, is still not fully understood. A clear key point is that the I-phase power threshold can play a role in the access to H-mode.

In the last decades, the L-H transition has been intensively studied. Using biased electrodes [17] and input heating power, the L-H transition has been realized successfully. The L-H transition induced by sawtooth heat pulses has also been studied [18]. Recently, the zonal flow's role as a trigger event or initiator has been detected during the I-phase or before the L-H transition in many devices [8-9]. However, the L-I transition, particularly the free I transition induced by a sawtooth heat pulse, has not been studied. The turbulent bursts during the I-phase have also not been reported. This is important, since the bursty character of the I-phase turbulence reveals aspects of the coupled zonal flow-turbulence dynamics.

In this paper, we report the first experimental evidence of LCOs triggered by sawtooth heat pulses in the HL-2A tokamak plasmas. As a heat pulse arrives at the edge plasmas and modulates edge gradients, the transition from L-mode to LCOs occurs. The statistical distribution of delay time shows that the L-I transition usually lags relative to sawtooth crashes by about 0.5ms. During the LCO, the turbulence become bursty, and the zonal flows and turbulence bursts all couple with the D_a oscillations. The zonal flows mainly modulate the LCO turbulence in the frequency band of ~20-100 kHz while turbulence with frequency higher than 100 kHz is more energetic in I-phase than L-mode. The turbulence lifetime (defined as the atuo-correlation time of the ambient turbulence (AT)) also becomes bursty in the I-phase. In addition, the power transfer between zonal flows, including geodesic acoustic modes (GAMs) [19-21], and turbulence are analyzed.

This paper is arranged as follows. Section 2 presents the experimental setup. The experimental results, including the triggering of LCOs by sawtooth heat pulses, simulation of the L-I transitions, sheared flow decorrelation of turbulence, statistical characteristics of electric fluctuations, phase changes and power transfer, etc, are described in section 3. The last section gives a brief summary.

2. **Experimental setup**

The experiments presented here were conducted in neutral-beam-injection (NBI) heated deuterium plasma of a single-null divertor configuration on the HL-2A tokamak. The major and minor radii of the HL-2A tokamak are R = 1.65m and a = 0.4 m, respectively. The NBI power is ~900 kW, close to the power threshold for L-H transitions. The parameters specially set for the experiments are the toroidal magnetic field $B_t \sim 1.35T$, the plasma current $I_p = 170 - 180 \, kA$, the line averaged electron density $N_e \sim 2 \times 10^{19} m^{-3}$, the safety factor $q_{95} \sim 3.8$. The digitizer can handle fluctuation data up to 500 kHz. A combination of distributed Langmuir probe (LP) arrays was used to measure floating potential fluctuations, density and temperature. In the combination, a 3x6 probe array yields density, temperature and turbulence stress data. A radial rake probe array of 12 tips and a four-tip LP array forming a fast reciprocating probe set of 16 tips with a 65 mm poloidal span were used to get profiles of floating potential and radial electric field. The probe arrays are inserted into the region 0.5-1.0cm inside the last closed flux surface (LCFS). The tip size and the mount of the LP sets are the same as was described in Ref [6, 21-22].

3. **Experiment results**

   3.1 **Triggering of LCOs by sawtooth heat pulses**

Following sawtooth crashes, the LCOs are detected in NBI-heated plasmas with heating power close to the power threshold for the L-H transition. Figures 1 (a)-(d) present the soft X-ray signals, D_α signals on the divertor plate, zonal potentials in the frequency band of 0.5-3kHz, and Mirnov signals, respectively. The duration of the sawtooth heat pulse is ~4-5ms. As the sawtooth crash occurs at ~699.2ms, the heat pulse propagating to the edge plasma modulates the edge gradients. Following the sawtooth crash, the MHD activity first drops sharply [23-24], then D_α signals and zonal potentials all start to oscillate at the same frequency, which indicates that the plasma jumps from the L-mode into the LCO. At the L-I transition, the D_a signals

drop in a manner that is similar to the L-H transition induced by sawtooth heat pulses [18], but not as far. Compared with the H-mode case, the zonal potentials evolve and their frequencies decrease gradually. This observation suggests that the sawtooth heat pulse triggers the L-I transition.

A series of L-I transitions were also observed following sawtooth crash events at present heating power and where the LCOs tend to return to L-mode. The intensity of sawtooth crashes is defined as $\Delta I / I_0$. Here, ΔI and I_0 are the variation of Soft X-ray intensity during sawtooth crashes and the averaged intensity, respectively. However, for small sawtooth crashes of $\Delta I / I_0 < 0.35$, the L-I transition did not occur. Figures 2 (a) and (b) show the intensity of Soft X-Ray and D_α signals. Note that the L-I transitions usually lag behind sawtooth crashes. To understand the relation between sawteeth and L-I transitions, the delay time is analyzed further. Figure 3 provides the probability distribution function (PDF) of the delay time for the L-I transitions with respect to sawooth crashes. Here, we count the delay time for more than 60 sawtooth crashes which lead L-I transitions. The most probable delay time between the sawtooth crashes and onset of the LCOs is found to be slightly less than ~1ms.

3. 2 Simulation of L-I transitions induced by heat pulses

The L-I transition triggered by heat pulses was simulated by using a 1D reduced model [12]. In this two predators (zonal flow and mean flow)-one prey (turbulence) model, the zonal flow was found to be an important player in the L-H transition. This is because the zonal flow mediates the transition and reduces the power threshold, relative to a model where the zonal flow is heavily damped. The zonal flows can store fluctuation energy without increasing transport, and thus allow the mean flow shear to increase, so the transition can develop. Figure 4 shows the simulation results for an L-I transition induced by a single heat pulse at t=2.0x10^5(a/C$_s$). The LCO appears at t~2.1x10^5(a/C$_s$) after the single pulse is induced. Once the LCO is excited it tends to be long-lived. In contrast, with a lower heat power, an intrinsic I-L back transition is

observed as shown in figure 5. A heat pulse is induced at t=5x10^4(a/C$_s$), after a while the LCO appears at t=6 x10^4(a/C$_s$). However, the LCO damps slowly and the system returns to the L-mode finally. From this model, the observed LCO in the L-I-L experiments may be a damped oscillation of the zonal flow at lower heating power.

3.3 Sheared flow decorrelation of turbulence during limit cycle oscillations

The time evolutions of D$_ą$ signals, the turbulence intensity, turbulent decorrelation rate, $E \times B$ flow shearing rate of less than 3 kHz when the plasma stays in an I-phase are studied to understand the role of the sheared flows in regulating the turbulence in the LCO regime. Figures 6 (a)-(d) show the D$_ą$ signals, turbulence intensity, turbulence decorrelation rates γ_{dc}, and $E \times B$ flow shearing rates $\gamma_{E\times B} = dV_{E\times B}/dr$, respectively. Here, the turbulence decorrelation rate is estimated with the auto-correlation function analysis and the turbulence is selected in the frequency band of 30-400 kHz. The D$_ą$ signals follow turbulence with a phase shift about π/2, indicating that turbulence transport indeed leads to the D$_ą$ burst. The $E \times B$ flow shearing rate $\gamma_{E\times B}$ is higher than the turbulence decorrelation rate during the LCO and out of phase with turbulence intensity. In addition, the phase shift between shearing rates and decorrelation rates is close to zero.

3.4 Statistical characteristics of electric fluctuations during limit cycle oscillations

In order to get more detailed information about zonal flows and turbulence during the limit cycle oscillations, the statistical characteristics of potential fluctuations are investigated. Figures 7 (a)-(d) provide the spectrograms for the potential fluctuations during the L-I transition, lifetime of turbulence, average power of turbulence in the frequency band of 20-500kHz, and root mean square amplitudes of turbulence in the frequency bands of 20-100kHz and 100-400 kHz, respectively. During the LCOs, turbulent bursts and the significant zonal flow appear. Between bursts, turbulence is reduced significantly. The intensity of bursty turbulence, particularly that of the high

frequency part of the spectra (>100 kHz), can be significantly stronger than that of the L-mode. However, the average power of the LCO turbulence is comparable with that of L-modes. The result suggests that the bursty turbulence of higher intensity drives the zonal flows. Here, 'bursty' refers to the turbulent state where the turbulence intensity and lifetime periodically increase by roughly 10 times and 2 times, respectively, very rapidly in the I-phase.

However, the averaged root mean square amplitudes for the LCO turbulence in the frequency band of ~20-100 kHz are lower than that observed in the L-mode. In contrast, the averaged root mean square amplitudes of turbulence in the frequency band of 100-400 kHz during the LCO are higher than that of the L-mode. These suggest that the zonal flows mainly modulate turbulence in the frequency band of ~20-100 kHz but the LCO turbulence with frequency more than 100 kHz have more power than that of the L-mode. The power spectra of the floating potential fluctuations in the L-mode and I-phase plasmas are also studied and described in Figure 8. During the L-mode, a peak in the frequency at ~12 kHz is the potential fluctuations associated with the tearing mode of m/n=4/1[23, 24]. Here, the m and n are poloidal and toroidal mode numbers, respectively. After the plasma enters into I-phase, the MHD activity disappears, and the power of the zonal flows or fluctuations of frequency less than 10 kHz increase. The power of the turbulence with frequency higher than 20 kHz and less than 100 kHz during the L-mode is higher than that in the I-phase, but the power of turbulence with frequency higher than 100 kHz is lower in the L-mode plasmas. The results suggest that the intermediate range of frequencies loses energy to the zonal flow at the onset of I-phase [7]. The energy increase in the higher frequency fluctuations (>100kHz) during LCO could be attributed to the high frequency regime gaining the energy from the intermediate range of frequencies through nonlinear three wave coupling [7, 25]. Related to shearing, the power transfer between turbulence and zonal flows will be discussed in section 3.5 below.

The lifetime of turbulence in the frequency band of 30-400 kHz is also estimated with time window of 25μs with the auto-correlation function analyses. The lifetime of

the turbulence during the I-phase is shorter than that of the L-mode. In addition, the lifetime also becomes bursty during the LCO, as shown in Figure 7 (b). The auto-correlation functions of turbulence in the frequency band ~30-400 kHz are also given in Figure 9 (a). Compared with the L-mode case, the auto-correlation time τ_{AC} of turbulence drops to ~2μs and the coherency significantly decreases. The results suggest that the zonal flow shears decorrelate turbulence. Figure 9 (b) shows the auto-correlation function of the bursty and weak turbulence using conditional average analysis. The coherency of the weak turbulence is significantly lower than that of the bursty turbulence. Considering that the decrease of the auto-correlation time during the LCO possibly comes from the increase of the sheared $E \times B$ advection rather than the increased zonal flow shearing rates, the drift time $l_\theta / V_{E \times B}$ of turbulence eddies due to the $E \times B$ flow is estimated. Here, l_θ and $V_{E \times B}$ are the poloidal correlation length of turbulence and $E \times B$ drift velocity, respectively. During the I-phase, the measured lifetime of turbulence is less than 2μs. The turbulence poloidal correlation length l_θ is evaluated as ~2cm, and the zonal flow velocities are less than 1×10^4m/s. We find $l_\theta / V_{E \times B} > \tau_{AC}$. Thus, the decrease of the turbulence lifetime and its burst during the LCO is because the increased zonal flow shearing rates decorrelate turbulent eddies.

3. 5 Phase shifts between turbulence and zonal flows in L-mode and I-phase

The phase shifts among turbulence, zonal flows and D_a signals in the L-mode are compared with those observed in the I-phase. Figure 10 shows the time evolutions of the soft X-ray signals (a), D_a signals (b), turbulent intensity (c) and zonal potentials (d). Before the L-I transition, no correlation between the turbulence and D_a signals is detected, but zonal flows are anti-phase correlated with turbulence. Following the sawtooth crash, turbulence and zonal flows are all correlated with D_a signals. The zonal flows lag behind the turbulence by about π/2 after the sawtooth crash ~1.8ms, in significant contrast with the observation in L-mode.

3.6. Power transfer between turbulence and zonal flows

The time resolved power transfer between turbulence and zonal flow is estimated during the LCOs. Figure 11 shows the zonal flow velocities (a), the perpendicular kinetic energy of the turbulence (b), Reynolds stresses (c), zonal flow energy production (d), and the rates of energy transfer (e). The stresses are calculated with $R_S = \langle v_\theta v_r \rangle$. Here, v_θ and v_r are the poloidal and radial turbulent velocities, computed from the high frequency components from the turbulence. <..> is the time average over a suitably time period of 10μs that lies bewteen the LCO oscillation period (~300-500μs) and the turbulent autocorrelation time (~2-3μs). The turbulent stresses in the frequency band of ~0.5-3kHz are 180 degrees out of phase with the zonal flows, suggesting that the oscillatory stresses perform work on the zonal flow. The zonal flow energy production and the rate of energy transfer resulting from the stresses are evaluated by $R'_S V_{ZF}$ and $R'_S V_{ZF} / V_\perp^2$. Here, R'_S, V_{ZF} and $V_\perp^2$ are the stress gradient, zonal flow velocity and perpendicular kinetic energy of the turbulence, respectively. As the energy transfer production reaches its peak, the absolute amplitudes of the zonal flows reach their maximum. At the same time, the rate of energy transfer also peaks. The result is consistent with the measurement which show that the power transfer is from the turbulence to the zonal flows. However, the cycle, phase relations, and theoretical expectations suggest a two-way transfer at different points of the cycle, but we do not know that from this analysis.

For comparison, the power transfer between turbulence and GAMs is also analyzed in Ohmic plasmas. Similar properties of the instantaneous energy transfer between turbulence and GAMs are also detected. Figure 12 gives (a) the GAM velocity, (b) the perpendicular kinetic energy of turbulence, (c) the turbulent Reynolds stresses, (d) GAM energy production (e), and the rate of energy transfer (f). The GAM is anti-phase correlated with the turbulence intensity and stresses. The GAM energy production frequency is double of the GAM frequency and the positive peaks correspond to the maximum or minimum of the GAM velocity. The rates of the

energy transfer are in-phase with the energy transfer production. The analyses indicate that the turbulent stresses also perform work on the GAM and the power transfer is from the turbulence to the GAM.

4. Summary

Limit cycle oscillations induced by sawtooth heat pulses are studied using multiple Langmuir probe arrays in the edge plasmas of the HL-2A tokamak for the first time. The sawtooth heat pulse propagates to the plasma boundary and modulates the edge gradients, then the transition from L-mode to LCOs occurs. During the I-phase, the zonal flow, turbulence and D_a signal oscillate at the same frequency. A series of L-I-L transitions induced by sawtooth heat pulses are also detected. Results from the 1D model suggest the LCO at lower heating power may be a kind of damped oscillation. The statistical analyses show that the most probable delay time between the sawtooth crash and onset of the LCO is slightly less than ~1ms. The intensity of bursty turbulence in the I-phase is stronger than that observed in the L-mode plasmas. The lifetime of the LCO turbulence shortens in comparison with that in L-mode. The zonal flows regulate the low frequency turbulence of 20-100 kHz, while the turbulence of frequency higher than 100 kHz has higher power than that measured in the L-mode. The phase shifts between turbulence and zonal flows change from π (L-mode) to $\pi/2$ (after the onset of the LCOs ~1.8ms). The analysis of time-resolved power transfer suggests the power transfer exists between turbulence and zonal flows. The direction of the power transfer is from turbulence into geodesic acoustic modes in ohmic plasmas.

Reference

[1] Wagner F et al 1982 Phys. Rev. Lett, **49**, 1408.

[2] Biglari H et al 1990 Phys. Fluids, **B2**, 1.

[3] Diamond P H et al 2005 Plasma Phys. Cont. Fusion, **47**, R35.

[4] Hasegawa. A et al 1987 Phys. Rev. Lett. **59**, 1581.

[5] Fujisawa A et al 2004, Phys. Rev. Lett. **93**,165002.

[6] Zhao K J et al 2010 Plasma Phys. Cont. Fusion, **52**, 124008.

[7] M Xu et al 2012 Phys. Rev. Lett. **108** 245001.

[8] Estrada T et al 2011 Phys. Rev. Lett. **107**,245004.

[9] Schmitz L et al 2012 Phys. Rev. Lett. **108**, 155002.

[10] Conway, G. D et al 2011 Phys. Rev. Lett. 1**06,** 065001.

[11] Colchin R J, et al Nucl. Fusion **42**, 1134 (2002).

[12] Zohm H et al Phys. Rev. Lett, **72**, 222(1994).

[13] Hubbard A E et al Nucl. Fusion **52**, 114009 (2012).

[14] Kim E J and Diamond P H, 2003 Phys. Rev. Lett , **90**, 185006.

[15] Miki K and Diamond P H 2012 Phys. Plasmas **19** 092306.

[16] Manz P et al 2012 Plasma Phys **19** 072311.

[17] Van Milligan B Ph et al 2011 Nucl. Fusion **51** 113002.

[18] Wagner F et al 1984 Phys. Rev. Lett, **53**, 1453.

[19] Winsor N et al 1968 Phys. Fluids, **11**, 2448.

[20] McKee G R et al 2003 Phys. Plasmas, **10**, 1712.

[21] Zhao K J et al 2006 Phys. Rev. Lett. **96**, 255004.

[22] Yan L W et al 2006 Rev.Sci. Instrum, **77**, 113501.

[23] D. Biskamp, Magnetic Reconnection in Plasmas, (Cambridge University Press, Cambridge, England, 2000).

[24] Kaw P K, Valeo E J, and Rutherford P H, Phys. Rev.Lett. **43**, 1398 (1979).

[25] Zhao K J et al, Nucl. Fusion **49** 085027 (2009).
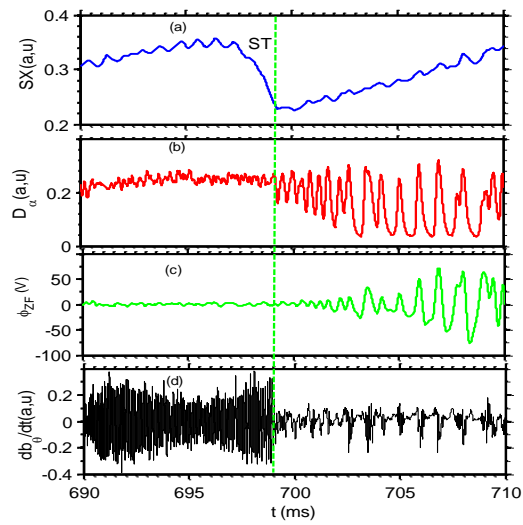
Fig.1 Following the sawooth (ST) crash (a), heat pulse propagates to the edge, then D_a signals (b) and zonal potentials (c) oscillate at the same frequency, and MHD sharply drops (d).
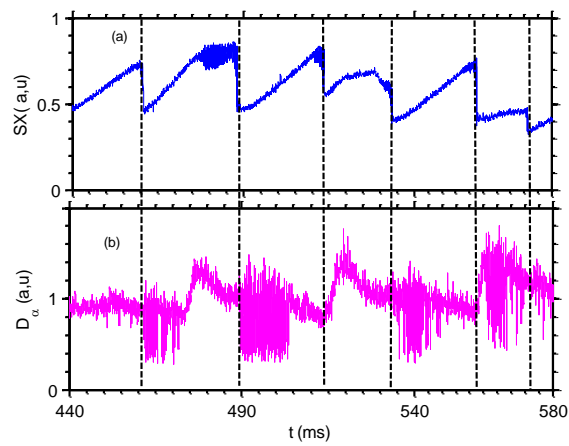

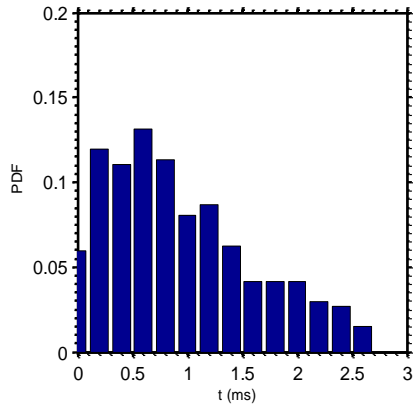Fig. 2 (a) The intensity of soft X-ray, (b) D_a signals.

Fig. 3 The probability distribution function of the delay time for the L-I transition, following sawtooth crashes.
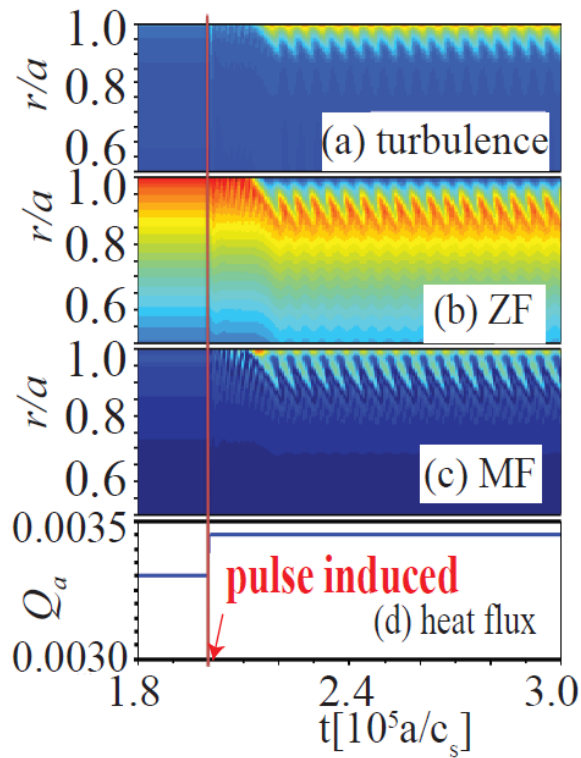

Fig. 4 Simulation of the L-I transition induced by a heat pulse. (a) Turbulent intensity, (b) zonal flow intensity, (c) mean flows, (d) mean heat flux.
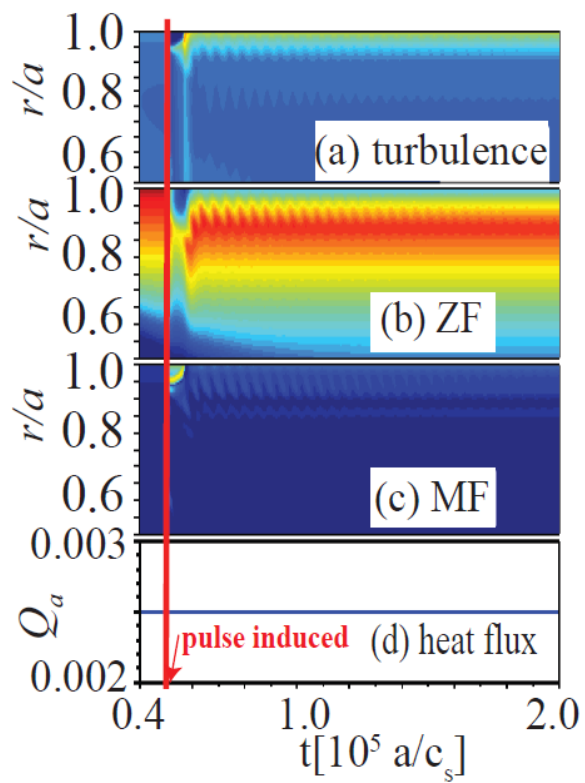
Fig. 5 Simulation of the intrinsic I-L back transition. (a) Turbulent intensity, (b) zonal flow intensity, (c) mean flows, (d) mean heat flux.
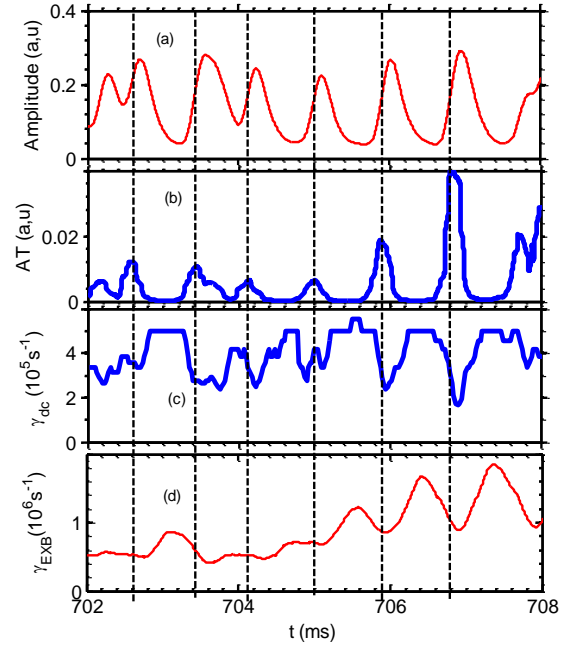
Fig. 6. From top to the bottom, (a) D$_a$ signals, (b) intensity of ambient turbulence, (c) turbulent decorrelation rates, and (d) ExB flow shearing rates.
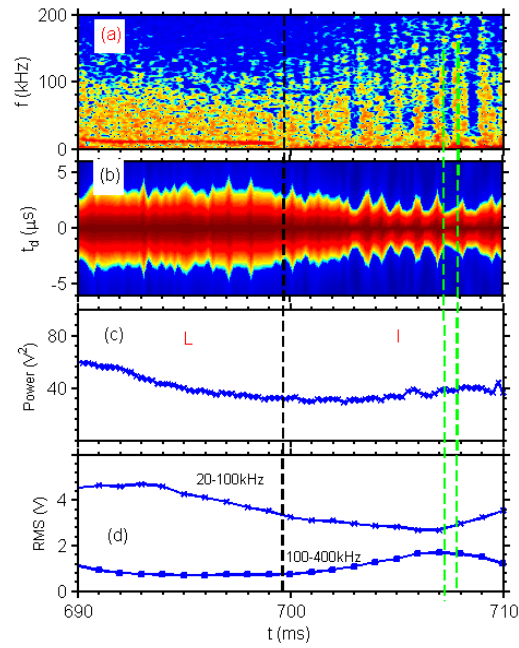
Fig 7 (a) The time evolutions of potential fluctuations of the L-I transition, (b) lifetime of turbulence, (c) averaged power of turbulence at the frequency band of 20-500kHz, and (d) root mean square amplitudes of turbulence at the frequency bands of 20-100kHz and 100-400kHz.
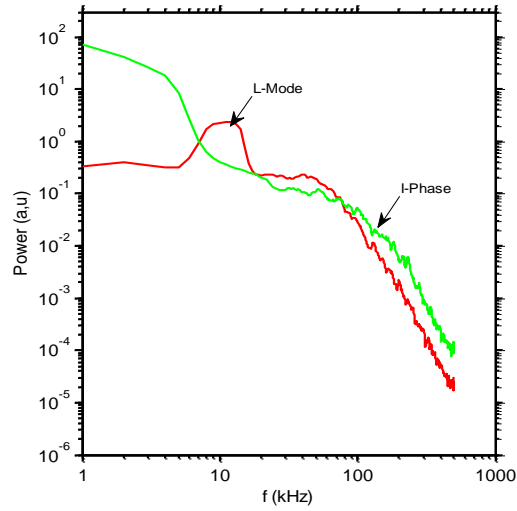
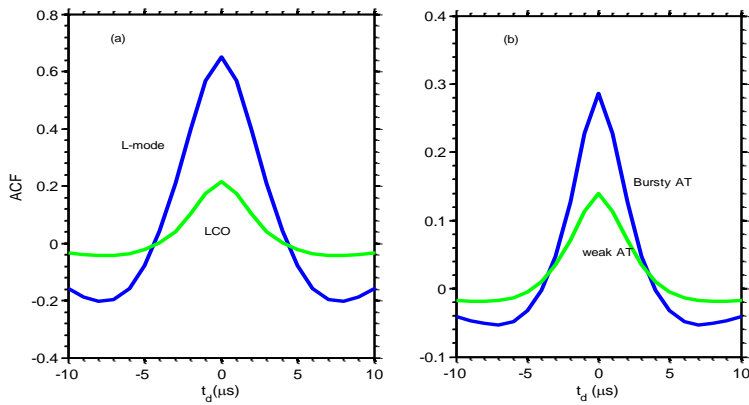Fig 8 The power spectra of potential fluctuations during the L-mode and I-phase plasmas.

Fig. 9 (a) Auto-correlation functions of turbulence during L-mode and limit cycle oscillations, (b) auto-correlation functions of turbulence during the bursty and weak components of the I-phase turbulence.
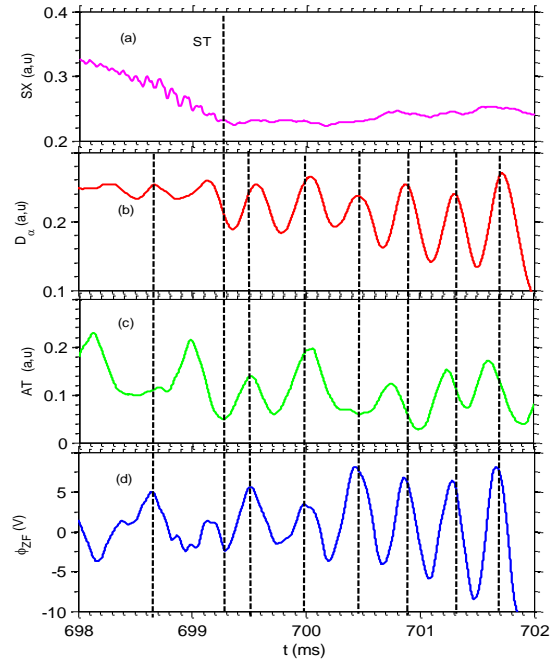
Fig. 10 The time evolutions of soft X-ray (SX) signals
(a), D_α signals (b), turbulent intensity (c) and zonal
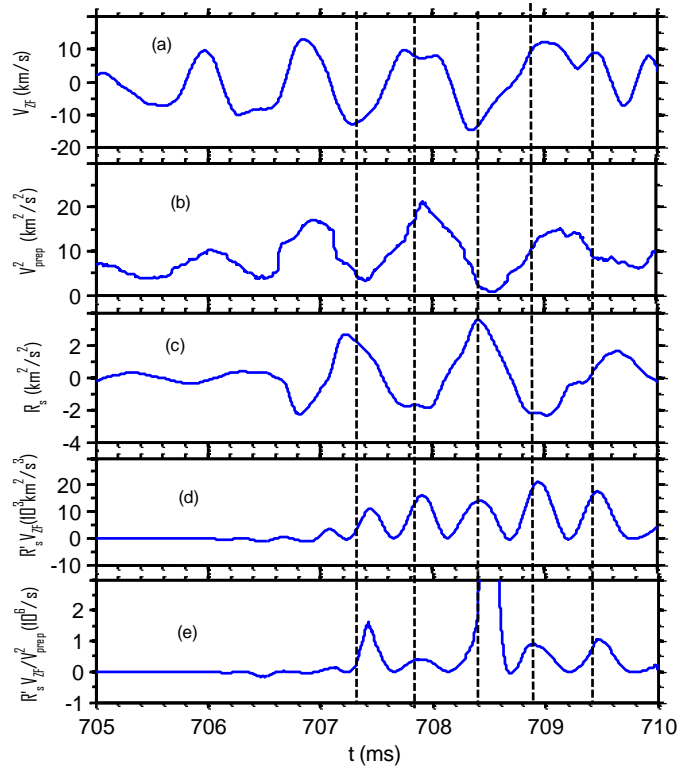potentials ϕ_{ZF} (d).

Fig. 11. From top to bottom, (a) zonal flow velocities, (b) the perpendicular kinetic energy of turbulence, (c) Reynolds stresses, (d) zonal flow energy production, (e) and the rates of energy transfer.
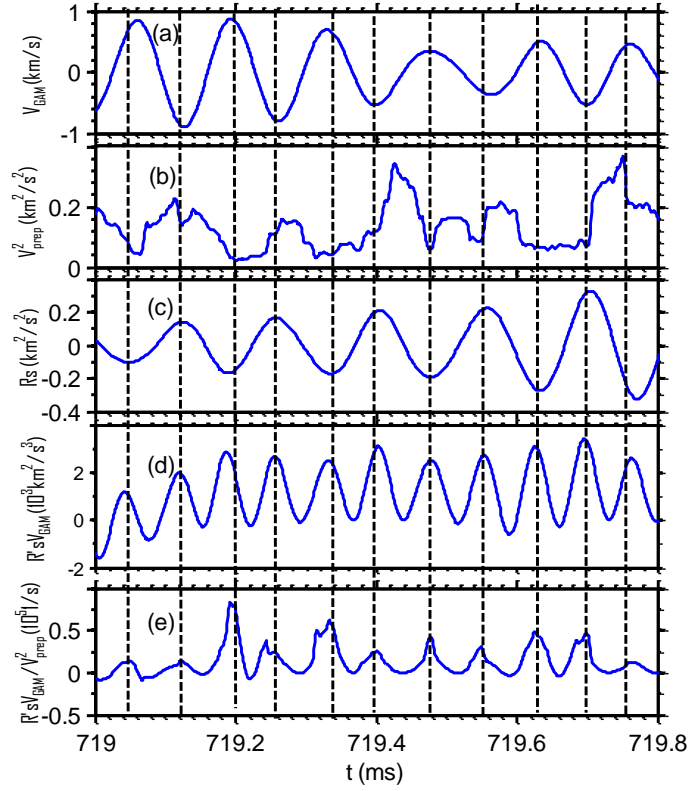
Fig. 12 From top to bottom, (a) GAM velocities, (b) the perpendicular movement energy of turbulence, (c) Reynolds stresses, (d) GAM energy production, and (e) the rates of energy transfer.